Design Procedure for Stable Operations of First-Order Reaction Systems in a CSTR

Johan J. Heiszwolf and Jan M. H. Fortuin
Dept. of Chemical Engineering, University of Amsterdam, 1018 WV, Amsterdam, The Netherlands

An application-oriented design procedure is presented for unique and point-stable operations of first-order reaction systems in a continuous stirred-tank reactor (CSTR). For a given set of values of kinetic constants, reaction enthalpy, feed conditions, residence time, and relevant physical properties, two boundary values of the heat-transfer capacity (St_1, St_3) and two of the modified coolant temperature ($\theta_{mc,2}$, $\theta_{mc,3}$) are analytically derived after a linearization of the unsteady mass and energy balances. With these boundary values, two separate design conditions are formulated; one for the heat-transfer capacity (HTC, characterized by St) and one for the modified coolant temperature (MCT, characterized by θ_{mc}). Each of these conditions is sufficient to guarantee unique and point-stable steady-state operations for a range of St or θ_{mc} values. Predicted behaviors of reacting systems are compared with experimental results obtained from five different systems reacting in four bench-scale and two commercial reactors.

Introduction

In the process industry, unstable steady states and sustained oscillations of temperature and composition of reacting systems have generally to be avoided. These undesired phenomena may adversely affect product quality and downstream operations, and can lead to difficult process control and unsafe reactor operations. Therefore, it is important to know which values of the coolant temperature and the heat-transfer capacity will lead to unique and point-stable steady states, because these states show the desired behaviors of reacting systems. Since 1953 many papers (e.g., Van Heerden, 1953; Bilous and Amundson, 1955; Uppal et al., 1974; Farr and Aris, 1986) and overviews (Schmitz, 1975; Razon and Schmitz, 1987) concerning nonlinear behaviors of reacting systems have been published. However, in most of these articles predicted and observed reactor behaviors are not compared and quantitative agreement between predicted and measured results can only be found in a small number of selected articles (Vleeschhouwer and Fortuin, 1990). Further, such a comparison often requires familiarity with bifurcation and/or singularity theory (Scott, 1993) and the use of complex numerical analysis. Moreover, it has to be noted that for a given set of values of kinetic constants, adiabatic temperature rise, and residence time, the separate effect of the coolant temperature and that of the heat-transfer capacity on the behavior of the reacting system cannot easily be shown, because both the Arrhenius temperature and the adiabatic temperature rise are mostly made dimensionless with a reference temperature containing the temperature of the coolant and/or that of the feed.

In the present article, an easily applicable design procedure is presented using a constant reference temperature ($T_o = T_A/\kappa$), which is a chosen fraction of the Arrhenius temperature. The stability criteria are derived from a set of five relationships (Eqs. 13 to 17) between key parameters (Da, Δ_a, St, θ_{mc}). This set of relationships, which holds for three critical steady states, is obtained after a linearization of the unsteady mass and energy balances. The values of the four key numbers and the additional Lewis number (Le) which are defined in the Notation section, fix the type of steady state. These numbers have been defined in such a way that a range of values of the coolant temperature (T_c) and that of the heat-transfer capacity (φUS), resulting in unique and point-stable operations, can be obtained for each combination of values of kinetic constants, adiabatic temperature rise, residence time, and relevant physical properties (Da, Δ_a, Le).

The procedure is applied to five different first-order reaction systems in four bench-scale (0.24–0.50 L) and two commercial reactors (6,000 L). Predicted and observed behaviors of these systems are compared in the "Application" section.

Correspondence concerning this article should be addressed to J. M. H. Fortuin.

Process-Engineering Model

The behavior of a first-order reaction system in a continuous stirred-tank reactor (CSTR) will be described with a process-engineering model, which means that the model can be used for design and operation and that each of the parameters has a physical meaning and a physically acceptable value that can be determined in a separate experiment (Fortuin, 1970). The model consists of the following material and energy balances that contain dimensionless physical quantities, that is, the three variables temperature (θ), conversion (ξ), and time (τ) and the six parameters representing the residence time (Da), the adiabatic temperature rise (Δ_a), the heat-transfer capacity (St), the modified coolant temperature (θ_{mc}), a ratio of heat capacities (Le), and an arbitrary number (κ).

$$\frac{d\xi}{d\tau} = -\xi + Da(1-\xi)\exp\left[\kappa - \frac{\kappa}{\theta}\right] \equiv f_1$$

(Material balance) (1)

$$\frac{d\theta}{d\tau} = -\frac{(1+St)}{Le}(\theta - \theta_{mc}) + \frac{\Delta_a}{Le}Da(1-\xi)\exp\left[\kappa - \frac{\kappa}{\theta}\right] \equiv f_2$$

(Energy balance). (2)

The definition of the parameters in Eqs. 1 and 2 differ from those in "classic models" (Uppal et al., 1974; Ray and Hastings, 1980; Farr and Aris, 1986) in which the temperature of the reacting system is made dimensionless by using a reference temperature containing the temperature of the coolant and/or that of the feed. In the present article, the following procedure is applied.

The feed temperature T_f, the inlet coolant temperature $T_{c,i}$, and a constant physical heat production ΔQ are combined into the modified coolant temperature T_{mc}. Further, the temperatures and times of the dimension holding balances are made dimensionless with a constant reference temperature $T_o = T_A/\kappa$ and a characteristic reaction time used as a reference time $t_O = k^{-1}\exp(\kappa)$, in which κ has an *arbitrary* chosen value. As a result, $\theta_{mc} = T_{mc}/T_O$, and each of the remaining parameters Da, Δ_a, St, and Le is independent of T_{mc}.

These definitions are applied in order to be able to show the separate effects of the heat-transfer capacity (HTC, characterized by St) and the modified coolant temperature (MCT, characterized by θ_{mc}) on the behavior of first-order reaction systems for a fixed set of values of Da, Δ_a, and Le. With regard to the five dimensionless parameters in Eqs. 1 and 2, it may be stated that two of them can be considered as ratios of times ($Da = t_R/t_O$; $St = t_R/t_N$), two as ratios of temperature ($\Delta_a = \Delta_a T/T_O$; $\theta_{mc} = T_{mc}/T_O$), and one as a ratio of heat capacities ($Le = (m_L C_{P,L} + m_w C_{P,W})/(m_L C_{P,F})$).

Behavior of Reacting System

For steady-state conditions ($f_1 = f_2 = 0$), Eqs. 1 and 2 yield Eq. 3, which is represented by the S-shaped curves in Figure 1 for 19 different St values. The S-shaped curves in Figure 1 are the loci of points representing steady states of first-order reaction systems in a CSTR for a given set of values of Da, Δ_a, and Le. Each S-shaped curve is associated with a fixed value of St. For a steady state, the following equation holds:

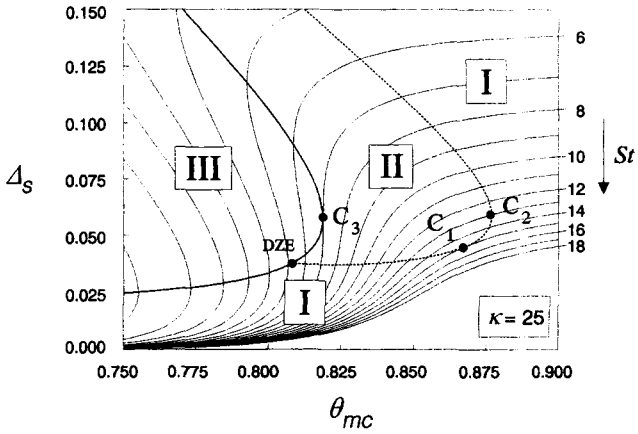

Figure 1. S-shaped curves obtained with Eqs. 3 and 4 for 19 different values of *St* and fixed values of *Da*=30, Δ_a=0.982694, *Le*=1.5, and κ=25.

The dashed line is the *bifurcation curve* (Eq. 8); the bold line represents the *slope curve* (Eq. 9). The points C_1, C_2, and C_3 refer to critical steady states. The three regions cover point-stable (I), orbitally stable (II), and unstable (III) steady states.

$$\theta_{mc} = \frac{\kappa}{\kappa + \ln\left[Da\left(\frac{\Delta_m}{\Delta_s} - 1\right)\right]} - \Delta_s \qquad \text{(S-shaped curve)}, \quad (3)$$

in which

$$\Delta_s = \theta_s - \theta_{mc} \qquad \text{and} \qquad \Delta_m = \frac{\Delta_a}{1+St}. \quad (4)$$

After differentiation of Eqs. 1 and 2 with respect to ξ and θ, substitution of $f_1 = 0$, $f_2 = 0$, $\xi = \xi_s$, and $\theta = \theta_s$ and elimination of the steady-state conversion ξ_s by applying Eqs. 1 to 4, the following equation for the Jacobian J is obtained:

$$J \equiv \begin{bmatrix} \frac{df_1}{d\xi} & \frac{df_1}{d\theta} \\ \frac{df_2}{d\xi} & \frac{df_2}{d\theta} \end{bmatrix} = \begin{bmatrix} \frac{-\Delta_m}{\Delta_m - \Delta_s} & \frac{\Delta_s \kappa}{\Delta_m \theta_s^2} \\ \frac{-\Delta_s}{\Delta_m - \Delta_s}\frac{\Delta_a}{Le} & \frac{\Delta_a}{\Delta_m Le}\left(\frac{\Delta_s \kappa}{\theta_s^2} - 1\right) \end{bmatrix}. \quad (5)$$

With the Jacobian J, the time-dependent behavior of infinitesimally small perturbations ($\delta\xi$, $\delta\theta$) applied at steady-state conditions, can be calculated. The trace and the determinant of the Jacobian J associated with Eqs. 1 and 2 are given by

$$\mathrm{tr}J = \frac{\Delta_a}{Le\Delta_m}\left[\frac{\kappa\Delta_s}{(\Delta_s + \theta_{mc})^2} - 1\right] - \frac{1}{1 - \Delta_s/\Delta_m} \qquad \text{(Trace)} \quad (6)$$

$$\det J = \frac{1+St}{Le(1-\Delta_s/\Delta_m)}\left[1 - \frac{\kappa\Delta_s(1-\Delta_s/\Delta_m)}{(\Delta_s + \theta_{mc})^2}\right]$$

(Determinant). (7)

For each complete set of numbers (Da, Le, St, Δ_a, θ_{mc}, and κ), the type of steady state can be determined with Eqs. 3, 4, 6, and 7. A *point-stable* steady state is obtained, if both the slope condition, det $J > 0$ (Van Heerden, 1953), *and* the dynamic condition, tr $J < 0$ (Bilous and Amundson, 1955), hold. Substituting tr $J = 0$ and det $J = 0$ into Eqs. 6 and 7 and eliminating St using Eqs. 3 and 4 yield Eqs. 8 and 9, represented by the dashed *bifurcation curve* and the bold *slope curve* in Figure 1. These sign-changing lines are the loci of points on S-shaped curves where the sign of tr J and that of det J change.

$$(\theta_{mc})_{\mathrm{tr}=0} = \theta_s - \left[\frac{\kappa}{\theta_s^2} - \frac{2Le}{\Delta_a}\left\{1+\cosh\left(\frac{\kappa}{\theta_s} - \kappa - \ln(Da)\right)\right\}\right]^{-1} \quad \text{(Bifurcation curve)} \quad (8)$$

$$(\theta_{mc})_{\det=0} = \theta_s - \frac{\theta_s^2}{\kappa}\left[1 + Da\exp\left(\kappa - \frac{\kappa}{\theta_s}\right)\right] \quad \text{(Slope curve)} \quad (9)$$

The slope curve is the locus of points representing neutral stable steady states.

In Figure 1, the two sign-changing lines divide the diagram into three regions:

- Region I (tr$J < 0 <$ det J), in which all points refer to point-stable steady states.
- Region II (tr $J > 0 <$ det J), in which the steady states are orbitally stable. This means that after an infinitesimally small perturbation of such a steady state, the relationship between the concentration ξ and the temperature θ will not approach a single point, but a closed loop or orbital in a ξ, θ diagram (Vermeulen et al., 1986). Then the behavior of the reaction system will result in sustained oscillations of temperature and composition in time. These types of behavior are also referred to as limit cycles. For each orbitally stable steady state represented by a point on an S-shaped curve in Region II, the extreme values of the temperature rise, which can numerically be calculated with Eqs. 1 to 4, can considerably exceed Δ_m (Vermeulen et al., 1986). In the worst case, the maximum temperature rise of these cycles is limited by the adiabatic temperature rise Δ_a.
- Region III (det $J <$ 0), in which the steady states are unstable. After an infinitesimally small perturbation, each steady state represented by a point on an S-shaped curve in Region III will result in a transition to a point-stable or orbitally stable one. This transition can also numerically be calculated with Eqs. 1 to 4.

In the next section, it will be shown that for given values of Da, Δ_a, and Le unique and point-stable steady states are always obtained, if St exceeds two critical St values *or* θ_{mc} exceeds two critical θ_{mc} values.

Critical Steady States

In Figure 1, the S-shaped curve with $St = St_1$ has a contact point C_1 with the bifurcation curve. This contact point is called a *degenerate Hopf-bifurcation* point, since two Hopf points coincide (Scott, 1993). It is obvious that all steady states represented by points located on the S-shaped curves with $St > St_1$ satisfy the dynamic condition, independent of the value of θ_{mc}. For the steady state represented by point C_1 ($\theta_{mc,1}$; $\Delta_{s,1}$) of the S-shaped curve with $St = St_1$, the following equations hold:

$$\theta_{mc,1} = (\theta_{mc})_{\mathrm{tr}=0} \quad \text{and} \quad \left[\frac{\partial\theta_{mc}}{\partial\Delta_s}\right]_1 = \left[\frac{\partial\theta_{mc}}{\partial\Delta_s}\right]_{\mathrm{tr}=0} \quad \text{(Steady state } C_1\text{)}. \quad (10)$$

Further, it is clear that for the steady state represented by point C_2 ($\theta_{mc,2}$; $\Delta_{s,2}$) in Figure 1, the following equations are valid:

$$\theta_{mc,2} = (\theta_{mc})_{\mathrm{tr}=0} \quad \text{and} \quad \left[\frac{\partial\theta_{mc}}{\partial\Delta_s}\right]_{\mathrm{tr}=0} = 0 \quad \text{(Steady state } C_2\text{)}. \quad (11)$$

Figure 1 shows that for all steady states with $\theta_{mc} > \theta_{mc,2}$ the dynamic condition is also satisfied. Moreover, one S-shaped curve in Figure 1 has a contact point with the slope curve. This point is referred to as a *cusp catastrophe* (Scott, 1993; Drazin, 1994). It is evident that in Figure 1 all steady states represented by points located on the S-shaped curves to the right of C_3, that is, curves with $St > St_3$, are always *unique* so that no unstable steady states can occur, independent of the value of θ_{mc}. For the steady state represented by point C_3 ($\theta_{mc,3}$; $\Delta_{s,3}$), the following equations hold:

$$\theta_{mc,3} = (\theta_{mc})_{\det=0} \quad \text{and} \quad \left[\frac{\partial\theta_{mc}}{\partial\Delta_s}\right]_{\det=0} = 0 \text{ (Steady state } C_3\text{)}. \quad (12)$$

Using Eqs. 3, 4 and 8 to 12, the following *key-number relationships* can analytically be derived for three critical steady states represented by

- Point C_1:

$$Da = \left[\frac{\Delta_a}{\kappa Le}\left(-1+\sqrt{1+\frac{\kappa Le}{\Delta_a}}\right) \times\left\{-1+\sqrt{1+\frac{\kappa Le}{\Delta_a}\left(1+\frac{1+St_1}{Le}\right)}\right\}\right] \times\exp\left[\left\{\sqrt{1+\frac{\kappa Le}{\Delta_a}}+\sqrt{1+\frac{\kappa Le}{\Delta_a}\left(1+\frac{1+St_1}{Le}\right)}\right\}-\kappa\right]. \quad (13)$$

- Point C_2:

$$\frac{\kappa}{\theta_{s,2}^2} - \frac{2Le}{\Delta_a}\left(1+\cosh\left(\frac{\kappa}{\theta_{s,2}} - \kappa - \ln Da\right)\right) - \frac{1}{\theta_{s,2}}\left(\frac{2\kappa}{\theta_{s,2}} - \frac{2Le\kappa}{\Delta_a}\sinh\left(\frac{\kappa}{\theta_{s,2}} - \kappa - \ln Da\right)\right)^{0.5} = 0 \quad (14)$$

$$\theta_{mc,2} = \theta_{s,2}\left[1-\left\{\frac{2\kappa}{\theta_{s,2}}-\frac{2Le\kappa}{\Delta_a}\sinh\left(\frac{\kappa}{\theta_{s,2}}-\kappa-\ln Da\right)\right\}^{-0.5}\right]. \quad (15)$$

- Point C_3:

$$Da=\left[1-\frac{2\Delta_a}{\kappa(1+St_3)}\left\{\sqrt{\kappa\frac{1+St_3}{\Delta_a}+1}-1\right\}\right]\times\exp\left[2\left\{\kappa\frac{1+St_3}{\Delta_a}+1\right\}^{0.5}-\kappa\right] \quad (16)$$

$$Da=\left(1-\frac{4\theta_{mc,3}}{\kappa}\right)\exp\left(\frac{\kappa}{\theta_{mc,3}}-2-\kappa\right). \quad (17)$$

From Eqs. 13 to 17, four boundary values (St_1, St_3, $\theta_{mc,2}$, and $\theta_{mc,3}$) can be calculated, from which two simplified conditions can be derived, that is, an HTC condition and an MCT condition. The HTC condition includes St_1 from Eq. 13 and St_3 from Eq. 16. The MCT condition contains $\theta_{mc,2}$ from Eqs. 14 and 15 and $\theta_{mc,3}$ from Eq. 17.

In the next section, it is shown that these conditions are applicable to all first-order reaction systems in a CSTR and that either the HTC or the MCT condition is *sufficient* to obtain unique and point-stable steady states. With respect to the points C_1, C_2, and C_3 of Figure 1, it can be added that the relative location of these points can change for a different set of values of Da, Δ_a, and Le as is shown in Figure 2.

Design Procedure

The values of US and $T_{c,i}$ for unique and point-stable operations are derived in this section. If the values of fourteen relevant physical quantities (c_f; $C_{p,c}$; $C_{p,f}$; $C_{p,L}$; $C_{p,w}$; $(-\Delta H)$; ΔQ; k; m_L; m_w; T_A; T_f; $\Phi_{m,c}$; $\Phi_{m,f}$) are known and a suitable value of κ, for example, $\kappa = 25$, is chosen, the values of the numbers Da, Δ_a, and Le can be calculated with the definitions in the Notation section. For a conservative design of a reactor, the value $Le = 1$ has to be preferred. Substituting the values of these numbers into Eqs. 13 to 17 yields the values of St_1, St_3, $\theta_{mc,2}$, and $\theta_{mc,3}$. Then *unique* and *point-stable* steady states are always obtained if St or θ_{mc} is chosen in such a way that *one* of the following conditions holds:

$$\bullet\ St_1 < St > St_3 \qquad \text{(HTC condition)} \quad (18)$$

or

$$\bullet\ \theta_{mc,2} < \theta_{mc} > \theta_{mc,3} \qquad \text{(MCT condition)}. \quad (19)$$

Each of these conditions is *sufficient* for obtaining unique and point-stable steady-states of a first-order reaction system in a CSTR. If $St = St^*$ satisfies the HTC condition, the required value $(US)^*$ of the heat-transfer capacity, based on the local overall heat-transfer coefficient U, follows from:

$$[US]^* = -\Phi_{m,c}C_{p,c}\ln\left(1-\frac{\Phi_{m,f}C_{p,f}}{\Phi_{m,c}C_{p,c}}St^*\right). \quad (20)$$

The connection between US and the dimensions of the reactor and its accessories is elucidated in the Appendix.

If $\theta_{mc} = \theta^*_{mc}$ satisfies the MCT condition, the required value of the inlet coolant temperature follows from:

$$T^*_{c,i} = \theta^*_{mc}T_0 + \frac{1}{St^*}\left(\theta^*_{mc}T_0 - T_f - \frac{\Delta Q}{\Phi_{m,f}C_{p.f}}\right). \quad (21)$$

If application of the HTC or MCT condition results in unsuitable values of the heat-transfer capacity or the inlet coolant temperature, the residence time (Da) and/or the feed conditions (Δ_a) can be changed and the boundary values updated, until the procedure results in *suitable* values of the four key numbers.

If neither the HTC nor the MCT condition can be satisfied, the boundaries of regions in which the steady states are point stable (PS), orbitally stable (OS), or unstable, can be calculated using the coordinates of the intersection points of the sign-changing lines (Eqs. 8 and 9) with the S-shaped curves (Eq. 3). In addition, it may be stated that with Eqs. 3, 6, and 7, for each set of parameter values, it can be investigated whether the classic necessary and sufficient Van Heerden–Amundson condition:

$$\text{tr}\,\boldsymbol{J} < 0 < \det \boldsymbol{J} \quad (22)$$

for point-stable (PS) steady states is satisfied.

A worst-case scenario, for example, due to failure of the stirrer resulting in a loss of the heat-transfer capacity ($St \to 0$), can be accounted for by considering the adiabatic temperature rise Δ_a only. Even, if temperature oscillations or excitation as a result of multiple steady states occur, the reactor temperature can never exceed:

$$\theta_{\max} = \theta_{mc} + \Delta_a \quad \text{or}$$

$$T_{\max} = T_f + \Delta Q/(\Phi_{m,f}C_{p,f}) + (-\Delta H)c_f/C_{p,f}. \quad (23)$$

Application

The design procedure outlined previously is applied to experimental data of four bench-scale reactors (A, B, C, D) and two commercial reactors (E, F), each containing one of the following pseudo-first-order reaction systems:

(A) Hydration of 1,2-epoxy propane; liquid phase (Antic et al., 1977)

(B) Hydration of 2,3-epoxy propanol; liquid phase (Vleeschhouwer et al., 1988)

(C) Hydrolysis of acetic anhydride; liquid phase (Haldar and Rao, 1991)

(D) Decomposition of hydrogen peroxide; liquid phase, gas formation (Wirges, 1980)

(E) Oxo reaction; gas/liquid phase (Vleeschhouwer et al., 1992)

(F) Oxo reaction; gas/liquid phase (Vleeschhouwer et al., 1992).

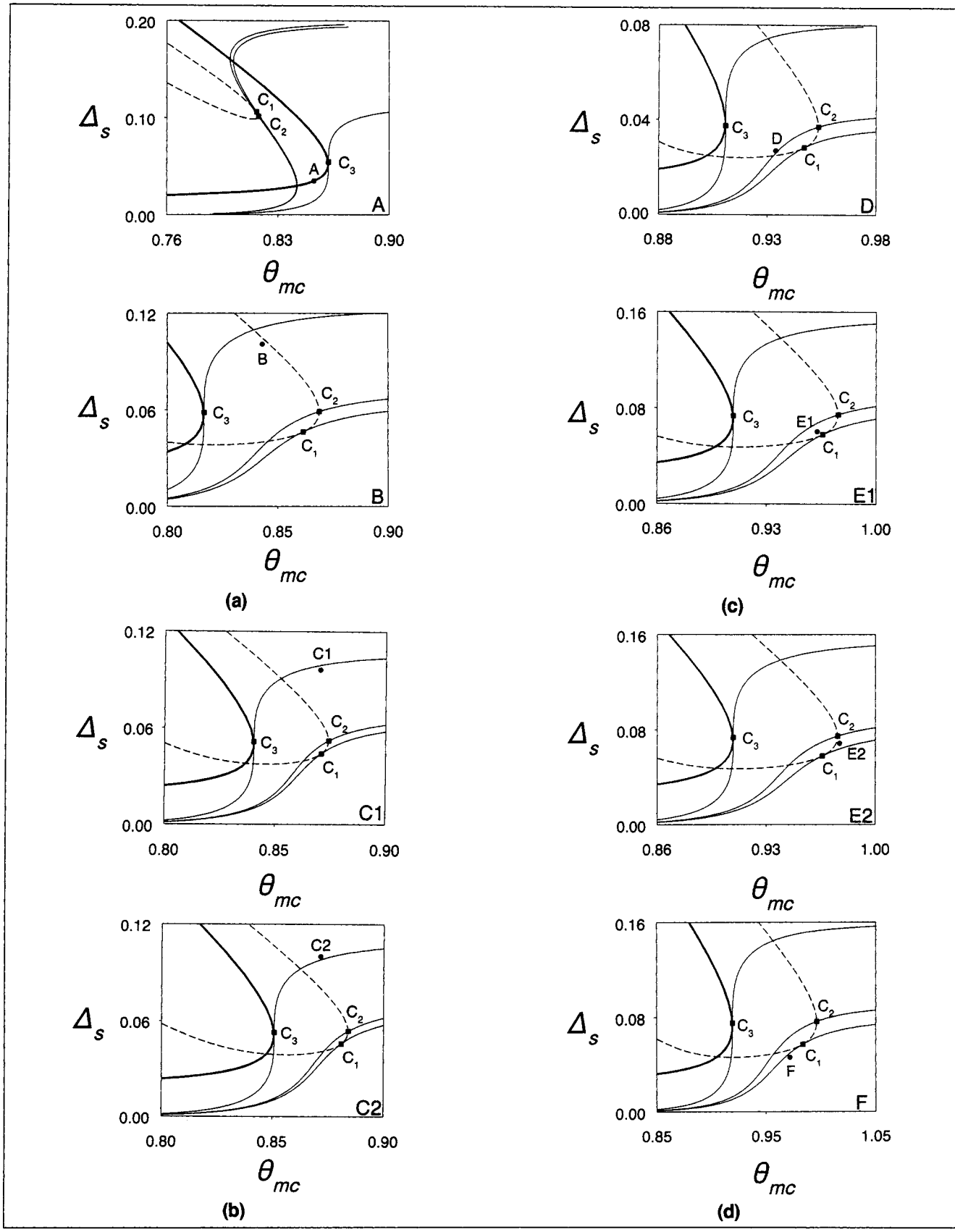

Figure 2. In each map of Figure 2, the operating point (●), the dashed bifurcation curve (Eq. 8), the solid slope curve (Eq. 9), and three S-shaped curves (Eq. 3) associated with the relevant set of critical steady states C_1, C_2, and C_3 (■) are shown; these maps correspond to the reacting systems *A* to *F* of Table 2.

Table 1. Relevant Physical Quantities of Five Different Reacting Systems in a CSTR: Four Bench-Scale Reactors (A, B, C, D) and Two Commercial Reactors (E, F)

Physical Quantity*	Reaction Systems							
	A	B	$C1$	$C2$	D	$E1$	$E2$	F
c_f	1.696	8.60	6.211	6.189	6.745	7.81	7.81	9.42
C_p	3,210	2,374	2,444	2,449	4,200	2,400	2,400	2,400
C_{pf}	3,210	2,469	2,444	2,449	4,200	2,700	2,700	2,700
$(-\Delta H)$	89.20×10^3	88.17×10^3	58.62×10^3	58.62×10^3	94.8×10^3	159×10^3	159×10^3	159×10^3
k	5.54×10^{11}	1.40×10^{10}	5.20×10^{12}	3.43×10^{12}	2.91×10^{17}	9.7×10^7	9.7×10^7	6.1×10^7
m	0.224	0.30	0.290	0.290	0.50	3.38×10^3	3.38×10^3	3.38×10^3
$m_wC_{p,w}$	0	427.3	83.7	83.7	0	4.6×10^6	4.6×10^6	4.6×10^6
$\Phi_{m,f}$	7.92×10^{-4}	1.81×10^{-3}	3.94×10^{-3}	4.02×10^{-3}	4.06×10^{-4}	3.20	3.20	2.76
ΔQ	10.1	29.45	0	0	0	-175×10^3	-175×10^3	-175×10^3
T_A	9,060	8,822	11.24×10^3	11.24×10^3	14.61×10^3	11×10^3	11×10^3	11×10^3
$T_{c,i}$	293.65	300.63	325.65	326.45	—	436.15	443.15	437.15
T_f	249.80	270.18	327.35	326.85	—	303	303	303
T_{mc}	257.51	297.52	326.09	326.56	303.2	423.52	429.95	427.61
φUS	0.263	29.45	27.28	25.42**	16.73	$98\cdot10^3$	$98\cdot10^3$	$118\cdot10^3$

*The required SI units are given in the Notation section.
**See the Appendix.

Data of these systems were borrowed from the cited literature and collected in separate columns of Table 1. Each column of Table 2 shows the volume of the reactor and six dimensionless parameter values calculated with associated values of Table 1, using relevant definitions of the Notation section. Further, the values of tr J and det J, calculated with Eqs. 3, 6, and 7, have been added to the data of Table 2. Application of the Van Heerden–Amundson criterion (* of Table 2) results in predicted steady-state behaviors (PS or OS), that agree with observed ones, except those of reacting systems $C1$ and $C2$.

With respect to the HTC and MCT conditions, the following procedure is applied. From the values of Da, Δ_a, Le, and κ, the boundary values St_1, St_3, $\theta_{mc,2}$, and $\theta_{mc,3}$ were calcu-

Table 2. Dimensionless Parameters of Five Different Reacting Systems A to F in a CSTR; Predicted and Observed Steady States

Physical Quantity	Reaction Systems							
	A	B	$C1$	$C2$	D	$E1$	$E2$	F
Volume	0.24 L	0.27 L	0.27 L	0.27 L	0.50 L	6,000 L	6,000 L	6,000 L
Da	14.65	32.23	35.77	23.12	10.26	1.423	1.423	1.037
Δ_a	0.156	0.8703	0.3976	0.3954	0.469	1.045	1.045	1.261
Le	1	1.538	1.118	1.118	1	1.39	1.39	1.39
κ	30	25	30	30	45	25	25	25
St	0.103	6.590	2.833	2.582	9.811	11.34	11.34	15.85
θ_{mc}	0.8527	0.8431	0.8704	0.8716	0.9339	0.9625	0.9772	0.9718
tr J	−0.966	0.716	−6.483	−3.638	0.739	0.442	−0.219	−1.209
det J	0.0001	27.05	36.16	23.832	14.31	18.18	32.56	18.17
Predicted*	PS	OS	PS	PS	OS	OS	PS	PS
Observed	PS	OS	OS††	OS††	OS	OS	PS	PS
St_1	−0.202	12.50	5.218	4.907	11.72	11.96	11.97	15.12
St_3	0.394	6.090	2.749	2.632	4.846	5.760	5.759	6.953
$\theta_{mc,2}$	0.8178	0.8689	0.8743	0.8841	0.9536	0.9759	0.9759	0.9963
$\theta_{mc,3}$	0.8619	0.8167	0.8404	0.8508	0.9107	0.9088	0.9088	0.9193
$St-St_1$	+	−	−	−	−	−	−	+
$St-St_3$	−	+	+	−	+	+	+	+
$\theta_{mc}-\theta_{mc,2}$	+	−	−	−	−	−	+	−
$\theta_{mc}-\theta_{mc,3}$	−	+	+	+	+	+	+	+
Predicted**	PS/M	OS/U PS/U	OS/U PS/U	OS/U PS/U	OS/U PS/U	OS/U PS/U	PS/U	PS/U
Observed	PS/M	OS/U	OS/U††	OS/M††	OS/U	OS/U	PS/U	PS/U
Predicted†	PS/M	OS/U	PS/U	PS/U	OS/U	OS/U	PS/U	PS/U
Observed	PS/M	OS/U	OS/U††	OS/M††	OS/U	OS/U	PS/U	PS/U

*Van Heerden-Amundson criterion.
**Criterion of present article.
†Criterion of Figure 2.
††The discrepancy between predicted and observed behaviors of $C1$ and $C2$ is discussed in the Appendix.

lated with Eqs. 13 to 17 and substituted into columns A to F of Table 2. Application of the HTC criterion to St and the MCT criterion to θ_{mc} also result in predicted steady-state behaviors (** of Table 2) that agree with observed ones, except those of reacting systems $C1$ and $C2$.

In the maps of Figure 2, the steady states of reacting systems A to F of Table 2 are represented by solid circles (●) and the associated critical points C_1, C_2, and C_3 by solid squares (■). Each of the maps also contains three S-shaped curves (Eq. 3), associated with the three critical steady states, and further the dashed bifurcation curve (Eq. 8) and the solid slope curve (Eq. 9).

From the topography of the eight maps of Figure 2, the steady-state behaviors of systems A to F can easily be derived. The results are also represented in Table 2, in which these predicted steady-state behaviors (†) are compared with observed ones. Application of the three criteria of Table 2 shows that discrepancies between predicted and observed behaviors are only found for system C. This is discussed in the next section.

Discussion

With regard to reaction system $C2$ of Table 2, the value of φUS could not be found directly in the article of Haldar and Rao (1991). However, using the φUS value and the operating conditions of $C1$ in Table 1 and the given change in the coolant mass-flow rate, the approximate value of φUS of $C2$ could be calculated (see the Appendix), resulting in $St < St_3$.

However, for reaction system $C2$, it was found that $\theta_{mc,3} < \theta_{mc} < \theta_{mc,2}$ resulting in a predicted behavior OS/unique (U) or PS/U, which does not agree with the observed behavior OS/multiple (M). This difference may be attributed to a less accurate value of the HTC and/or unreliable values of the kinetic constants. The latter was already noticed by Haldar and Rao (1991).

Further, Table 2 shows that for the commercial reactor E, a small *decrease* of θ_{mc}, from steady state $E2$ to steady state $E1$, results in a change from a point-stable steady state to a steady state with sustained oscillations. The observed steady states of the commercial reacting systems E and F completely agree with the predicted ones. The good agreement between observed and predicted steady-state behaviors of the Oxo reaction systems E and F show that sustained temperature oscillations can occur spontaneously, if the steady state is represented by a point in Region II of Figure 1. Note that these types of oscillations, which were already qualitatively described by Dubil and Gaube (1973), should not be confused with oscillations occurring in isothermal Oxo reactors as a result of a complicated scheme of reaction kinetics (Falbe, 1980; Seelig, 1976). It must be noted that an accurate description of the behavior of a reacting system requires values of the kinetic constants of the pseudo-first-order reaction, which have been measured at *representative* operating conditions. This is necessary because the concentration of reactants and catalysts and types of solvents can also affect the order of the reaction and the values of the kinetic constants (Gold and Hilton, 1955; Bunton and Perry, 1960; Mitzner and Lemke, 1985).

It can be added that for non-first-order reaction systems, equations similar to Eqs. 10 to 12 can be evaluated numerically. It may be shown that, for fixed values of Da, Δ_a, Le, and κ, for example, the value of St_1 increases for reaction orders $n < 1$ and decreases for $n > 1$.

Conclusions

In the present article, two stability criteria are presented for design and operation of first-order reaction systems in a CSTR. It is shown that for given values of the kinetic constants, reaction heat, feed conditions, residence time, and relevant physical properties (Da, Δ_a, Le, κ), two boundary values (St_1, St_3) of the heat-transfer capacity St^* and two ($\theta_{mc,2}$, $\theta_{mc,3}$) of the modified coolant temperature θ^*_{mc} can be calculated with Eqs. 13 to 17.

Unique and point-stable operations will occur:

- If St^* satisfies $St_1 < St^* > St_3$ (HTC condition)

or

- If θ^*_{mc} satisfies $\theta_{mc,2} < \theta^*_{mc} > \theta_{mc,3}$ (MCT condition).

It should be noted that these conditions are sufficient but not necessary. Then, the heat-transfer capacity US^* *or* the inlet coolant temperature $T^*_{c,i}$ required for a stable operation can be calculated with Eqs. 20 and 21.

The stability criteria that have been applied to five different systems reacting in bench scale and commercial reactors lead to predicted behaviors that generally agree with observed ones. Moreover, it is confirmed that a *decrease* of the coolant temperature (e.g., to compensate for the effect of fouling) can result in a transition from a *point-stable* steady state to sustained oscillations, for example, the transition from steady state $E2$ to steady state $E1$ in Figure 2 (Vleeschhouwer et al., 1992), and that a *decrease* of the coolant mass-flow rate can result in a change from a unique operation to a multiple one (Haldar and Rao, 1991).

It is further shown that sustained temperature oscillations in Oxo rectors can quantitatively be explained with the present model including pseudo-first-order reaction kinetics, which was already qualitatively done by Dubil and Gaube (1973).

Comparison of predicted and observed reactor behaviors showed that reliable predictions of the type of steady state of a reacting system require not only a correct mathematical treatment of stability conditions but also sufficiently accurate and representative values of relevant physical quantities, more particularly the kinetic data (Haldar and Rao, 1991).

Notation

c = concentration of the key component, mol/kg
k = frequency factor of first-order reaction, 1/s
m = mass, kg
t = time, s
t_N = Newtonian cooling time, $\varphi US/(m_L C_{p,f})$, s
t_R = residence time, $m_L/\Phi_{m,f}$, s
T_{mc} = modified coolant temperature,

$$T_{mc} = T_{c,i} + \left(\frac{\Delta Q}{\phi_{m,f} C_{p,f}} + T_f - T_{c,i} \right)(1 - \mathrm{St}), k^{-1}$$

T_s = steady-state temperature of reacting system, K
$\Delta_a T$ = adiabatic temperature rise, $(-\Delta H) c_f / C_{p,f}$, K
$-\Delta H$ = heat of reaction, J/mol

ΔQ = heat produced by stirring and mixing minus a heat flow to the surroundings, W
Φ_m = mass-flow rate, kg/s

Dimensionless parameters

Δ_m = maximum temperature rise, $\Delta_a/(1+St)$
Δ_s = steady-state temperature rise, $\theta_s - \theta_{mc}$
θ = temperature of reacting system, T/T_o
θ_s = steady-state temperature of reacting system, T_s/T_o
ξ = conversion, $1 - c/c_f$
φ = efficiency factor (Eq. A3)
Da = Damköhler number, $(m_L/\Phi_{m,f})k\exp(-\kappa) = t_R/t_0$
n = reaction order
St = Stanton number, $\varphi US/(\Phi_{m,f}C_{p,f}) = t_R/t_N$

Indices

c = at coolant side
det = 0 at det $J = 0$
f = feed
L = liquid-phase reaction system at liquid side
s = steady state
tr = 0 at tr $J = 0$
w = reaction vessel and accessories
1,2,3 = critical steady states represented by points C_1, C_2, and C_3 located on S-shaped curves with constant values of St_1, St_2, and St_3, respectively
$*$ = design value

Literature Cited

Antic, B. M., A. H. Heemskerk, and W. R. Dammers, "The Hysteresis of Steady States in Continuous Stirred Flow Reactors," *Proc. K. Ned. Akad. Wet. Amsterdam*, **B 80**, 133 (1977).

Bilous, O., and N. R. Amundson, "Chemical Reactor Stability and Sensitivity," *AIChE J.*, **4**, 513 (1955).

Bunton, C. A., and S. G. Perry, "The Acid-catalysed Hydrolysis of Carboxylic Anhydrides," *J. Chem. Soc.*, 3070 (1960).

Drazin, P. G., *Nonlinear Systems*, Cambridge University Press, Cambridge, England, p. 54 (1994).

Dubil, H., and J. Gaube, "Dynamik and Regelung von Rührkessel-Reaktoren, erläutert am Beispiel der Oxo-Reaktion," *Chem. Ing. Techn.*, **45**, 529 (1973).

Falbe, J., *New Syntheses with Carbon Monoxide*, Springer-Verlag, Berlin (1980).

Farr, W. W., and R. Aris, "Yet Who Would Have Thought the Old Man to Have so Much Blood in Him?—Reflections on the Multiplicity of Steady States of the Stirred Tank Reactor," *Chem. Eng. Sci.*, **41**, 1385 (1986).

Fortuin, J. M. H., "Kinetics of and Parameter Estimation for the Treatment Steps in the Waste Heat Boiler and the Absorption Tower of the Nitric Acid Process," *Proc. ISCRE* 1, Chemical Reaction Engineering, K. B. Bischoff, ed., Advances in Chemistry Series, Vol. 109, ACS, Washington, DC, p. 545 (1972).

Gold, V., and J. Hilton, "The Hydrolysis of Acetic Anhydride: V. Catalysis by Strong Acids," *J. Chem. Soc.*, 843 (1955).

Haldar, R., and D. P. Rao, "Experimental Studies on Limit Cycle Behaviour of the Sulphuric Acid Catalysed Hydrolysis of Acetic Anhydride in a CSTR," *Chem. Eng. Sci.*, **46**, 1197 (1991).

Mitzner, R., and F. Lemke, "Lösungmittelabhängigkeit der Spontanhydrolyse von Essigsäureanhydrid," *Z. Chem.*, **25**, 406 (1985).

Perry, R. H., *Chemical Engineers' Handbook*, 50th ed., McGraw-Hill, New York, 10.16 (1984).

Ray, W. H., and S. P. Hastings, "The Influence of the Lewis Number on the Dynamics of Chemically Reacting Systems," *Chem. Eng. Sci.*, **35**, 589 (1980).

Razon, L. F., and R. A. Schmitz, "Multiplicities and Instabilities in Chemically Reacting Systems—A Review," *Chem. Eng. Sci.*, **42**, 1005 (1987).

Schmitz, R. A., "Multiplicity, Stability and Sensitivity of States in Chemically Reacting Systems—A Review," *Chemical Reaction Engineering Reviews*, H. M. Hulburt, ed., Advances in Chemistry Series, Vol. 148, ACS, Washington, DC, p. 156 (1975).

Scott, S. K., *Chemical Chaos*, Clarendon, Oxford, p. 44 (1993).

Seelig, F. F., "System-Theoretical Investigation of Possible Oscillatory States in the Hydroformulation Process in an Open Isothermal System," *Naturforsch. B*, **31B**(7), 929 (1976).

Uppal, A., W. H. Ray, and A. B. Poore, "On the Dynamic Behavior of Continuous Stirred Tank Reactors," *Chem. Eng. Sci.*, **29**, 967 (1974).

van Heerden, C., "Autothermic Processes," *Ind. Eng. Chem.*, **45**, 1242 (1953).

Vermeulen, D. P., and J. M. H. Fortuin, and A. G. Swenker, "Experimental Verification of a Model Describing Large Temperature Oscillations of a Limit-Cycle Approaching Liquid-Phase Reacting System in a CSTR," *Chem. Eng. Sci.*, **41**, 1291 (1986).

Vleeschhouwer, P. H. M., D. P. Vermeulen, and J. M. H. Fortuin, "Transient Behavior of a Chemically Reacting System in a CSTR," *AIChE J.*, **34**, 1736 (1988).

Vleeschhouwer, P. H. M., and J. M. H. Fortuin, "Theory and Experiments Concerning the Stability of a Reacting System in a CSTR," *AIChE J.*, **36**, 961 (1990).

Vleeschhouwer, P. H. M., R. D. Garton, and J. M. H. Fortuin, "Analysis of Limit Cycles in an industrial OXO Reactor," *Chem. Eng. Sci.*, **47**, 2547 (1992).

Weast, R. C., *Handbook of Chemistry and Physics*, 55th ed., CRC Press, E24, E26, F49 (1975).

Wirges, H. P., "Experimental Study of Self-Sustained Oscillations in a Stirred Tank Reactor," *Chem. Eng. Sci.*, **35**, 2141 (1980).

Appendix: Discussion of Effective Heat Transfer

The experiments $C1$ and $C2$ in Table 1 were conducted under similar operating conditions. Multiple steady states ($C2$) were observed after decreasing the coolant mass-flow rate, resulting in a decrease of the heat-transfer capacity. Unfortunately, the article of Haldar and Rao (1991) only mentions one φUS value. In the following, the effect of the coolant mass-flow rate and impeller speed on the φUS value is discussed. It is shown that the mentioned decrease of the coolant mass-flow rate is sufficient to cause a change in the heat-transfer capacity from $St > St_3$ to $St < St_3$.

The local overall heat-transfer coefficient U based on the external surface area S of the cooling coil, can be calculated from:

$$U = \frac{1}{\frac{1}{\alpha_L} + \frac{D}{2\lambda}\ln\left(\frac{D}{d}\right) + \frac{D}{\alpha_c d}}. \tag{A1}$$

Table A1 shows the descriptions and values of additional parameters. Assuming a homogeneous bulk temperature of the reacting system and accounting for a quasi-steady-state coolant temperature profile along the coil, the heat-removal flow, based on the inlet coolant temperature follows from:

$$\Phi_{m,c}C_{p,c}(T_{c,\text{out}} - T_{c,i}) = \varphi US(T - T_{c,i}), \tag{A2}$$

in which

$$\varphi = \frac{1 - \exp(-US/\Phi_{m,c}C_{p,c})}{US/\Phi_{m,c}C_{p,c}}. \tag{A3}$$

The partial heat-transfer coefficient α_c inside a helical coil can be calculated from (Perry, 1984):

$$Nu_c = 0.023 Re_c^{0.8} Pr_c^{0.333}\left(1 + 3.5\frac{d}{D_{\text{coil}}}\right); \quad Re_c > 10{,}000. \tag{A4}$$

Table A1. Physical Quantities of the Heat-Transfer Equipment for Reacting System *C1*

Parameter	Description	Value	Unit
A	Coefficient in Eq. A5	46.6×10^{-3}	1
$C_{p,L}$	Specific heat-reaction mixture*	2444	J/(kg·K)
$C_{p,c}$	Specific heat coolant†	4180	J/(kg·K)
D_{coil}	Coil diameter	50×10^{-3}	m
D	External tube diameter	3.06×10^{-3}	m
d	Internal tube diameter	2.5×10^{-3}	m
D_{imp}	Impeller diameter	30×10^{-3}	m
L	Length of cooling coil	2.1	m
N_{imp}	Stirring speed	18.33	s^{-1}
Nu_c	Nusselt number ($\alpha_c d/\lambda_c$)	111.2	1
Nu_L	Nusselt number ($\alpha_L D/\lambda_L$)	11.11	1
$n1$	Exponent in Eq. A5	2/3	1
$n2$	Exponent in Eq. A5	1/3	1
$n3$	Exponent in Eq. A5	0.14	1
Pr_c	Prandtl number ($C_{p,c}\eta_c/\lambda_c$)	3.39	1
Pr_L	Prandtl number ($C_{p,L}\eta_L/\lambda_L$)	4.89	1
Re_c	Reynolds number ($\rho_c v_c d/\eta_c$)	19.8×10^3	1
Re_L	Reynolds number ($\rho_L N_{imp} D_{imp}^2/\eta_L$)	17.4×10^3	1
v_c	Velocity in tube	4.18	m/s
S	External surface area coil ($S=\pi DL$)	20.2×10^{-3}	m^2
η_c	Viscosity Coolant†	5.204×10^{-4}	Pa·s
η_L	Viscosity reaction mixture††	1×10^{-3}	Pa·s
$\eta_{L,w}$	η_L at wall temperature	1×10^{-3}	Pa·s
λ_{coil}	Thermal conductivity coil**	16.74	W/(m·K)
λ_L	Thermal conductivity reaction mixture††	0.5	W/(m·K)
λ_c	Thermal conductivity coolant†	0.643	W/(m·K)
ρ_L	Density reaction mixture*	1053	kg/m^3
ρ_c	Density coolant†	988.1	kg/m^3

*Linear combination pure component data.
**Value for stainless steel 316 (Perry, 1984).
†Weast (1975).
††Estimated.

The external partial heat-transfer coefficient of the cooling coil is difficult to calculate *a priori*, since the reactor geometry has a large effect on this coefficient. Unless a standard reactor geometry is used, the value of the heat-transfer coefficient can only be determined experimentally or roughly estimated from a correlation.

Generally, the external partial heat-transfer coefficient α_L of the coil can be calculated using the Sieder-Tate equation:

$$Nu_L = A Re_L^{n1} Pr_L^{n2} \left(\frac{\eta_L}{\eta_{L,w}}\right)^{n3}, \qquad \text{(A5)}$$

in which values $n1 = 2/3$ and $n2 = 1/3$ are commonly used and $n3$ is generally of the order 0.14. Parameter A depends on the reactor geometry and dimensions of the reactor, which are not known exactly. However, since the dimensions and geometry are fixed, A should be approximately equal for experiments $C1$ and $C2$ in Table 1. Coefficient A was calculated using the operating conditions of $C1$, the dimensions of the reactor and accessories, Eqs. A1 to A5, the cited value of $\varphi US = 27.28$ W/K (at $N = 18.33$ s^{-1}), and assuming a constant viscosity ($\eta_L = \eta_{L,w}$). For experiment $C1$, $A = 0.04658$ was obtained, using the physical quantities listed in Table A1. Assuming constant transport properties, the effect of the coolant mass-flow rate and that of the impeller speed can now be calculated for experiment $C2$. Table A2 gives the results. It is clear that due to the decreased coolant mass-flow rate for experiment $C2$, $St < St_3$ holds. However, the condition $\theta_{mc} > \theta_{mc,3}$ predicts a unique steady state for $C2$, which does not agree with the experimentally found behavior. This result is probably due to insufficiently accurate data on the heat-transfer capacity and unreliable kinetic data of reacting system C.

Table A2. Heat-Transfer Capacities of Reacting Systems *C1* and *C2*

Parameter	$C1$	$C2$	Unit
N	1,100/60	1,450/60	s^{-1}
$\Phi_{m,c}$	$20.5\cdot10^{-3}$	$10.17\cdot10^{-3}$	kg/s
φUS	27.28	25.42	W/K
St	2.833	2.582	—

Manuscript received Aug. 1, 1996, and revision received Nov. 4, 1996.